JOURNAL OF MAGNETIC RESONANCE **131,** 39–45 (1998)
ARTICLE NO. MN971343

Pulsed ENDOR Studies at 95 GHz of the Triplet State of $^{13}C_{60}$

G. J. B. van den Berg,* D. J. van den Heuvel,* O. G. Poluektov,* I. Holleman,† G. Meijer,† and E. J. J. Groenen*,[1]

*Center for the Study of Excited States of Molecules, Huygens Laboratory, University of Leiden, P.O. Box 9504, 2300 RA Leiden, The Netherlands; and †Department of Molecular and Laser Physics, University of Nijmegen, Toernooiveld, 6525 ED Nijmegen, The Netherlands

Received July 1, 1997; revised November 17, 1997

Fully ^{13}C-enriched C_{60} has been investigated by pulsed electron-nuclear double-resonance (ENDOR) spectroscopy at W-band frequency at 1.2 K. For molecular C_{60} the ENDOR spectra reflect the distortion of the molecule upon triplet excitation, and the fine-structure parameter D is found to be negative. For a single crystal of C_{60} the ENDOR spectra characterize the triplet excitation as delocalized over a pair of neighboring C_{60} molecules.

INTRODUCTION

As long as fullerenes have been around, studies using magnetic resonance methods have contributed to our knowledge of this new form of carbon (*1*). Nuclear magnetic resonance (NMR) has been decisive in proving the highly symmetric, icosahedral structure of ground-state C_{60}. The observation of a single $^{13}C_{60}$ NMR line revealed the equivalence of all carbon atoms of C_{60} and in combination with the five resonances observed for C_{70} proved the cage structure of the fullerenes (*2*). On the other hand, electron paramagnetic resonance (EPR) showed the distortion and symmetry lowering of C_{60} upon electronic excitation through the observation of a zero-field splitting in the low-temperature EPR spectrum of the triplet state (*3*).

While the distortion of C_{60} upon excitation into the lowest triplet state T_0 is expected theoretically and has been observed, a description of the structure is not yet within reach and even the symmetry of C_{60} in T_0 is still under debate. The T_{2g} character of this triple state under I_h symmetry (*4*) implies that C_{60} is subject to a Jahn–Teller instability. Quantum-chemical calculations by Surján *et al.* (*5*), using an extended Hubbard Hamiltonian in combination with CNDO/S, predicted that molecular C_{60} upon excitation into the lowest triplet state distorts to a structure of D_{5d} symmetry. The next-lowest triplet state, calculated only 0.065 eV higher in energy, corresponded to a structure of D_{2h} symmetry. The structure of C_{60} in the lowest triplet state probably depends on the environment. For the simple-cubic phase of the crystal at low temperature, the site symmetry is only S_6 which is compatible with a D_{2h} but not with a D_{5d} symmetry of C_{60}.

The zero-field splitting between the triplet sublevels of molecular C_{60} was initially derived from EPR spectra under irradiation (*3*) and has amply been confirmed, among others by zero-field optically detected magnetic resonance leading to values of $|X| = 100 \pm 3$, $|Y| = 129 \pm 3$, and $|Z| = 229 \pm 3$ MHz ($|D| = 343.5 \pm 3$, $|E| = 14.5 \pm 3$ MHz) for C_{60} in frozen toluene solution (*6*). The inequality of X, Y, and Z would be compatible with a symmetry reduction upon excitation toward D_{2h}. In view of the fact that the difference between X and Y is only small, an interpretation in terms of a symmetry lowering toward D_{5d}, which would actually require $X = Y$, has been put forward (*7*). The sign of the zero-field parameters cannot be derived from EPR. Closs *et al.* (*8*) concluded to a negative sign of the zero-field parameter D for C_{60} assuming an analogy with C_{70} for which they argued for a negative D value (recent W-band experiments reveal that D is positive for triplet C_{70} (*9*)). Regev *et al.* (*10*) assumed D to be negative as well in their analysis of time-resolved EPR data. Electron-spin-echo-envelope-modulation (ESEEM) experiments for C_{60} in toluene by Grupp *et al.* (*7*) were interpreted in terms of a spin-density distribution from which the authors concluded to a positive value of D, while later theoretical work (*11*) suggested a negative value of D. The lineshape of time-resolved (*10*) and pulsed (*12*) EPR spectra of frozen solutions of C_{60} and its variation with temperature down even to 4 K has been described in terms of pseudorotation, i.e., tunneling between symmetry-equivalent Jahn–Teller distortions. From simulations of this lineshape, Grupp *et al.* concluded that C_{60} in toluene adopts D_{5d} symmetry upon excitation into T_0 (*12*).

For crystalline C_{60}, W-band electron-spin-echo-detected EPR (*13*) and photoluminescence spectroscopy (*14*) have revealed that upon optical excitation below 80 K a triplet exciton state is populated. The observed orientation of the principal axes of the fine-structure tensor of this triplet state with respect to the crystal axes showed that C_{60} in the crystal

[1] To whom correspondence should be addressed. Fax: +31-71-5275819. E-mail: mat@molphys.leidenuniv.nl.

1090-7807/98 $25.00

distorts to a structure of D_{2h} symmetry upon excitation. The extension of the exciton could not be established as the EPR data are compatible with an excitation delocalized over a pair as well as over a chain of C_{60} molecules.

To get more information on the triplet-state wavefunction, hyperfine studies should be most helpful. Because ^{12}C has no nuclear spin, one must rely on ^{13}C ($I = \frac{1}{2}$) in natural abundance (1.1%) or on ^{13}C-enriched C_{60}. From a simulation of the variation of the triplet EPR linewidth for C_{60} in methylcyclohexane at 200 K as a function of ^{13}C enrichment, Zhang *et al.* (*15*) derived a ^{13}C hyperfine coupling constant of 0.06 G. Grupp *et al.* (*7*) investigated ESEEM spectra of a frozen solution of 10% ^{13}C-enriched C_{60} in toluene at 4 K. They obtained the best description of their data through modeling of the spin-density distribution by a $\sin^2\theta$ function, where θ represents the angle between the fivefold rotation axis and the radius vector of a particular carbon atom for a C_{60} molecule distorted to D_{5d} symmetry.

We have set up a program that comprises both 95-GHz pulsed ENDOR and 9-GHz ESEEM studies of C_{60} and fully enriched $^{13}C_{60}$ in a decaline/cyclohexane glass and as single crystals. In principle, this allows a detailed investigation of the distortion of C_{60} upon triplet excitation and of the extension of the triplet exciton in the C_{60} crystal. While for icosahedral C_{60} all carbons are equivalent, each carrying a spin density of 1/60, symmetry lowering results, for example, in four and nine distinct carbon sites for C_{60} molecules of D_{5d} and D_{2h} symmetry, respectively. As regards the extension of the exciton, a delocalization over two or an ''infinite'' number of C_{60} molecules leads to distinctly different spin densities and, correspondingly, hyperfine interactions.

Here we report 95-GHz pulsed ENDOR spectra and present a preliminary discussion. We show that (i) for C_{60} in decaline/cyclohexane the triplet sublevel T_z is highest in energy (D is negative) and (ii) the crystal triplet concerns a miniexciton; i.e., the excitation is delocalized over two neighboring molecules that form a deep trap in the crystal.

EXPERIMENTAL

The method used to produce 99.1% enriched $^{13}C_{60}$ was described previously (*17*) and crystals were grown through sublimation. The W-band pulsed EPR/ENDOR experiments were performed on a homebuilt spectrometer at 1.2 K (*18*). Either a $^{13}C_{60}$ solution in decaline/cyclohexane (3:1, v/v) or a $^{13}C_{60}$ single crystal ($\sim 0.3 \times 0.3 \times 0.2$ mm) were transferred into a capillary tube which was mounted in a cylindrical cavity.

For the EPR/ENDOR experiments the solution was irradiated at 530 nm with 10-mJ pulses at a repetition rate of 10 Hz using a GWU-OPO-C355 laser which was pumped by the third harmonic of a Continuum Surelite I-10 Nd:YAG laser. For the crystal 5-mJ pulses of 680 nm were applied at a repetition rate of 10 Hz using a Quanta Ray PDL-1 dye laser pumped by the second harmonic of a Quanta Ray DCR-2 Nd:YAG laser. We estimate that in both cases less than 10% of the light reached the sample. In the ESE-detected EPR experiments the laser flash was followed by a two-pulse sequence $p_1-\tau-p_2$ with microwave pulses p_1 and p_2 of 70 ns and a delay time τ of 430 ns. The first microwave pulse followed 50 μs after the laser flash. Spectra were obtained by monitoring the echo height as a function of the applied magnetic field. Pulsed ENDOR experiments were performed using a three-pulse sequence $p_1-\tau-p_2-T-p_3$ with microwave pulses p_1, p_2, and p_3 of 100 ns each and delay times τ and T of 200 ns and 120 μs, respectively. During the time T an intense radiofrequency pulse of 100 μs was applied to the sample via a coil near the cavity. Spectra were obtained by monitoring the echo height while scanning the radiofrequency. The ENDOR effect amounted to a 15 and 5% decrease in the echo intensity at maximum for the crystal and the solution, respectively.

RESULTS

Figure 1a shows the 95-GHz ESE-detected EPR spectrum of a frozen solution of $^{13}C_{60}$ in decaline/cyclohexane at 1.2 K upon excitation at 530 nm. The asymmetrical shape of the spectrum as regards the low- and high-field sides, not visible at 9 GHz, derives from the anisotropy of the g tensor and corresponds to $g_{zz} - g_{xx}(g_{yy}) = 0.00116 \pm 0.00006$.

Pulsed ENDOR spectra have been measured at various positions in the EPR spectrum. Figure 1b illustrates four of these, taken at the magnetic fields corresponding to maximum absorption and emission and low- and high-field edges. The arrows indicate the ^{13}C Zeeman frequencies ν_Z at the

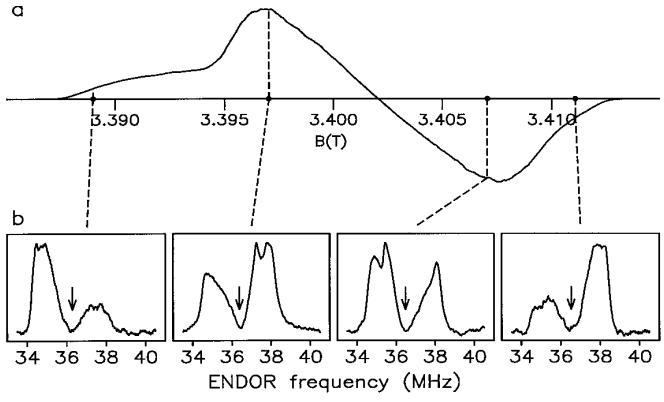

FIG. 1. ESE-detected EPR (a) and ^{13}C-pulsed ENDOR (b) spectra of $^{13}C_{60}$ in decaline/cyclohexane at 95 GHz and 1.2 K. The EPR signal is absorptive at low fields and emissive at high fields. The ENDOR spectra correspond to four different magnetic field settings and the arrows indicate the corresponding ^{13}C Zeeman frequencies.

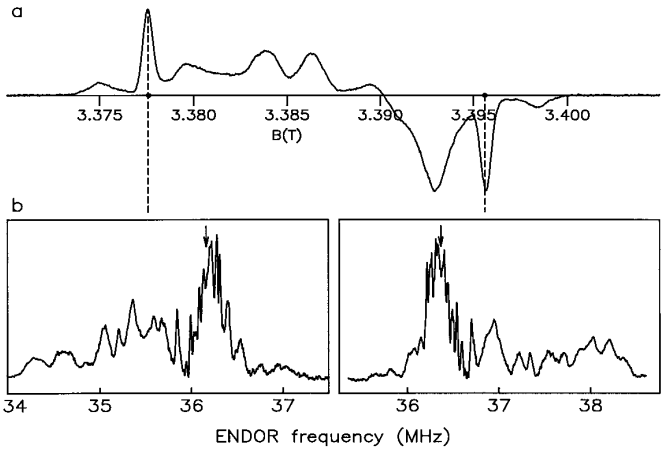

FIG. 2. ESE-detected EPR (a) and ^{13}C-pulsed ENDOR (b) spectra at 95 GHz and 1.2 K of a single crystal of $^{13}C_{60}$ for the magnetic field parallel to [110]. The ENDOR spectra are taken at fields of resonance of triplet γ. The arrows indicate the ^{13}C Zeeman frequencies.

magnetic field settings of the respective ENDOR experiments. The intensity distribution is determined not only by the hyperfine interaction but also to a considerable extent by the frequency dependence of the efficiency function F of pulsed ENDOR: $F(\nu) = \frac{1}{2}\sin^2[2\pi(\nu - \nu_Z)\tau]$ for $S = 1$, where τ represents the time between the first two microwave pulses (*19*). This efficiency function particularly explains the dip in the pulsed ENDOR spectra around ν_Z. The ENDOR spectrum spans a range of about 2 MHz on both sides of the Zeeman frequency. The intensity is distributed asymmetrically around ν_Z, in particular in the spectra corresponding to the lowest and highest magnetic fields. At these edges in the EPR spectrum, where only one of the triplet transitions contributes, ENDOR intensity is still observed on both sides of the Zeeman frequency. This implies that the hyperfine tensor must be largely anisotropic because otherwise the ENDOR shift would have the same sign for all atoms.

The 95-GHz ESE-detected EPR spectrum of a single crystal of $^{13}C_{60}$ for an orientation of the magnetic field parallel to a [110] axis upon excitation at 680 nm is shown in Fig. 2a. The narrow low- and high-field resonances correspond to stationary fields for this orientation of the magnetic field with respect to the crystal. Pulsed ENDOR spectra taken at these fields are represented in Fig. 2b. These spectra have not been recorded in a single radiofrequency scan. Each spectrum has been composed of about 10 spectra corresponding to frequency ranges of less than 1 MHz, which introduces some uncertainty as regards the intensity variation over the spectrum. For each part, the value of τ was adapted for maximum ENDOR efficiency. The ENDOR spectra reveal narrow lines close to the Zeeman frequency and broader lines further out, while the ENDOR intensity is distributed asymmetrically around the Zeeman frequency. At fields of about 3.4 T the high-field approximation applies, i.e., the ^{13}C Zeeman frequency is much larger than the hyperfine interaction, and the ENDOR spectra corresponding to the low- and high-field EPR transition are expected to be mirror images around the Zeeman frequency. The central part of the spectra fulfills this expectation, but in the outer parts some deviations occur.

DISCUSSION

The use of fully enriched $^{13}C_{60}$ and W-band pulsed EPR in combination with laser excitation has enabled ENDOR spectroscopy of the triplet state of molecular and crystalline C_{60}. The ENDOR spectra reflect the spin-density distribution over the fullerene and thereby represent fingerprints of the distortion upon optical excitation. A full analysis of these spectra based on quantum-chemical predictions of the triplet spin-density distribution for various geometrical structures is underway in our laboratory but is beyond the scope of the present paper. Here we will discuss the ENDOR spectra semiquantitatively in relation to two questions. First, what is the order of the triplet sublevels for molecular C_{60} in decaline/cyclohexane (i.e., the sign of D) and, second, how far does the triplet exciton extend for crystalline C_{60}?

The ENDOR frequencies are determined by the hyperfine interaction of the triplet electron spin with the ^{13}C nuclear spins of $^{13}C_{60}$. Because of the symmetry lowering of C_{60} upon excitation into the triplet state, the carbons are no longer equivalent which results in complex ENDOR spectra. As mentioned before, the spectra show that the hyperfine interaction is largely anisotropic. We therefore consider the contribution of the magnetic dipole–dipole interaction between the triplet electron spin, distributed over a C_{60} molecule, and a ^{13}C nuclear spin on atom i to the anisotropic hyperfine tensor which is given by

$$\overleftrightarrow{A}_i = \frac{\mu_0}{4\pi}\frac{1}{h} g_e \mu_B g_C \mu_N \sum_j \rho_j \left\langle \varphi_j \left| \frac{3\hat{r}\hat{r} - \overleftrightarrow{1}}{r^3} \right| \varphi_j \right\rangle . \qquad [1]$$

Here $\vec{r} \equiv \vec{r}_i - \vec{r}_e$, $r \equiv |\vec{r}|$, and $\hat{r} = \vec{r}/r$, and we assume the spin density ρ to be distributed over atomic orbitals φ_j. Two-center contributions (between the nuclear spin on atom i and the electron-spin density in φ_j on atom k, $k \neq i$) to the hyperfine interaction have been calculated (in a point-spin approximation) and found negligible compared to the one-center contributions for any reasonable spin-density distribution, which is understandable in view of the r^{-3} dependence of $\overleftrightarrow{A}$. The one-center integrals have been calculated as follows. In order to model the spatial distribution of the electron-spin density on atom i we have constructed four orthogonal hybrid orbitals out of the $2s$ and $2p$ atomic orbitals on atom i in such a way that three of these point along

the bonds toward neighboring atoms. In doing so we have adopted the icosahedral geometry of C_{60}. The fourth hybrid φ_i becomes an almost pure $2p$ orbital that makes an angle of 4.1° with the radial direction,

$$\varphi_i = 0.2840(2s)_i + 0.9564(2p_\xi)_i - 0.0681(2p_\eta)_i \quad [2]$$

in the local orthogonal axes system ξ, η, ζ on atom i defined by $\hat{\xi}$ along the radial direction, $\hat{\eta}$ in the plane of $\hat{\xi}$ and the interpentagon bond, and $\hat{\zeta}$ perpendicular to $\hat{\xi}$ and $\hat{\eta}$. We make the plausible assumption that all spin density on atom i is in orbital φ_i. Evaluation of the integral in Eq. [1] for φ_i, taking Slater-type $2s$ and $2p$ atomic orbitals with effective nuclear charge $Z = 3.45$, yields for spin density 1 in φ_i the following values for the elements of the anisotropic hyperfine tensor (*20*):

$$\begin{aligned} A_{\xi\xi} &= 167.6 \text{ MHz} \\ A_{\eta\eta} &= -83.2 \text{ MHz} \\ A_{\zeta\zeta} &= -84.4 \text{ MHz} \\ A_{\xi\eta} &= -17.9 \text{ MHz} \\ A_{\eta\zeta} &= A_{\zeta\xi} = 0 \text{ MHz}. \end{aligned} \quad [3]$$

This calculated tensor is consistent with the anisotropic hyperfine interaction observed for ^{13}C-containing radicals (*21, 22*).

From the sign of the tensor elements in Eq. [3] we conclude that the order of the triplet sublevels corresponds to $Z \gg X, Y$. Only a negative value of D reproduces the distribution of the ENDOR intensity above and below the ^{13}C nuclear Zeeman frequency observed in the spectra of Fig. 1b. The highest and lowest fields of resonance in the EPR spectrum of Fig. 1a derive from molecules for which the magnetic field is parallel to the principal z axis of the fine-structure tensor. For $D < 0$, the low-field transition corresponds to the $m_s = 0 \leftrightarrow m_s = -1$ transition and the ENDOR frequency for nucleus i is given by $\nu_Z + A_{zz}$. Because for most nuclei $\hat{z}$ is closer to $\hat{\eta}$, $\hat{\zeta}$ than to $\hat{\xi}$ and because $A_{\eta\eta}$ and $A_{\zeta\zeta}$ are negative, most nuclei will contribute to the ENDOR spectrum for frequencies smaller than ν_Z. This qualitative argument is corroborated by actual simulations for various spin-density distributions. In these simulations we had to add a small isotropic hyperfine interaction. We took the isotropic hyperfine interaction for each nucleus proportional to ρ_i and treated the proportionality constant (a_{iso}) as an adjustable parameter. In Fig. 3, we show a calculated ENDOR spectrum for a triplet molecule of icosahedral symmetry, i.e., with uniform spin-density distribution $\rho_i = \frac{1}{60}$, $i = 1, \ldots, 60$. Of course this distribution does not reflect the true spin densities and is inadequate for reproducing the experimental ENDOR spectrum. However, the ratio of the integrated intensities below and above the Zeeman frequency as calculated agrees with that in the experimental spectrum. Changing the order of the triplet sublevels would invert the spectrum with respect to the Zeeman frequency.

The second question we address concerns the extension of the triplet excitation of the crystal. Previously we have reported that optical excitation of a pure single crystal of C_{60} at helium temperatures populates triplet states not molecularly localized (*13*). Analysis of the ESE-detected EPR spectra at W band revealed the fine-structure tensor of these triplets and showed that the participating C_{60} molecules distort to D_{2h} symmetry, but did not allow a conclusion as regards the extension of the exciton over two neighboring molecules or over a linear chain of molecules. Photoluminescence experiments in combination with optical detection of magnetic resonance in zero field showed that these particular triplets are also responsible for a red phosphorescence of the crystal and according to their energy concern deep excitation traps (*14*). Initially we observed two distinct triplets, referred to as α and β, corresponding to different mutual orientations of the C_{60} molecules that form the exciton. Such orientations, the interpentagon bond facing a pentagon or a hexagon, respectively, were known to exist in the low-temperature simple-cubic C_{60} lattice. Later on additional ESE experiments showed the existence of a third triplet, γ, distinguishable from triplet β only in a magnetic field owing to the different orientation of the fine-structure principal axes of triplets β and γ with respect to the crystal axes. For the EPR spectrum in Fig. 2a, obtained for excitation of a single crystal at 680 nm and with the magnetic field parallel to [110], the relatively narrow low- and high-field bands corre-

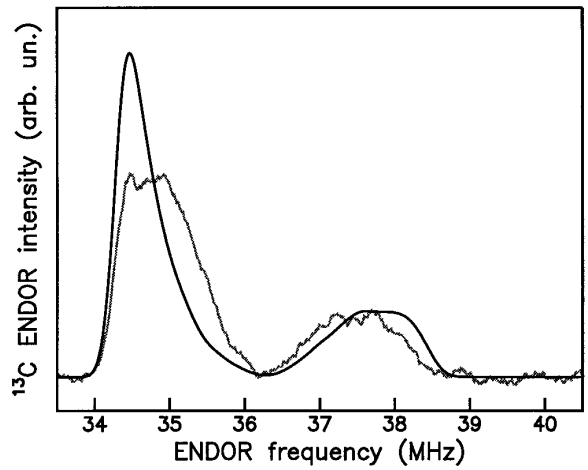

FIG. 3. Calculated ^{13}C-pulsed ENDOR spectrum at a magnetic field of 3.389 T for a hypothetical triplet $^{13}C_{60}$ molecule with uniform spin-density distribution. The isotropic hyperfine interaction parameter a_{iso} has been taken as −30 MHz (see text). For comparison the experimental spectrum at the same magnetic field (cf. Fig. 1) is reproduced in gray.

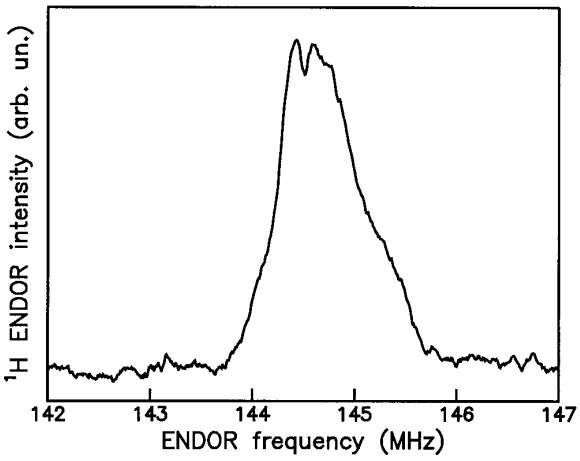

FIG. 4. ^{1}H-pulsed ENDOR spectrum at 1.2 K of a solution of $^{13}C_{60}$ in decaline/cyclohexane at 95 GHz and a magnetic field of 3.39 T.

spond to stationary fields of resonance of triplet γ. We will show that the pulsed ENDOR spectra taken at these fields, represented in Fig. 2b, allow a conclusion as regards the extension of the triplet excitons in the C_{60} crystal.

First, consider the narrow lines around ν_Z in the ENDOR spectra in Fig. 2b which may originate from ^{13}C nuclei of buckyballs neighboring the excited one(s). To check this hypothesis, we have measured the ^{1}H ENDOR spectrum of a frozen solution of C_{60} in a hydrocarbon solvent upon optical excitation (Fig. 4). The ENDOR intensity derives from solvent protons interacting with the triplet electron spin on C_{60}. The overall width of the ^{1}H spectrum amounts to about 2 MHz which, correcting for the difference in gyromagnetic ratio, limits the ^{13}C hyperfine interaction between neighboring buckyballs in the crystal to at most 0.5 MHz. Consequently, the narrow lines around ν_Z in the crystal spectra may partly derive from nuclei on neighboring C_{60} molecules, i.e., may concern matrix lines.

In the calculation of the pulsed ENDOR spectra for the C_{60} crystal, we consider C_{60} molecules of D_{2h} symmetry because ESE-detected EPR studies (*13*) have shown that the C_{60} molecules in the crystal distort in accordance with this symmetry upon excitation into the triplet exciton states α, β, or γ. We have adopted the molecular structure of D_{2h} symmetry as optimized by Surján *et al.* (*5*). The first step in the calculation concerns the spin-density distribution for a C_{60} molecule of this structure. A Hartree–Fock calculation has been performed in the MINDO approximation with the MOPAC 93 program (*23*), followed by a configuration-interaction calculation in the basis of the 15 singly excited triplet configurations constructed from the 5 degenerate highest occupied and 3 degenerate lowest unoccupied molecular orbitals. The calculated triplet state of lowest energy belongs to B_{1g} as found previously. For this state the calculated electron-spin densities on the atoms, i.e., the sum of the spin densities in the atomic orbitals, are listed in Table 1 and visualized in Fig. 5. The labels 1 to 9 refer to the inequivalent carbon positions in the buckyballs of D_{2h} symmetry. A rather uniform spin-density distribution has been obtained in which 85% of the spin density is spread over 56 atoms that have at most 2.3% spin density each. Only four atoms in one specific site carry a higher spin density of 3.7%.

Comparison of the width of the ^{13}C-pulsed ENDOR spectra of the crystal and the solution, Figs. 2b and 1b, respectively, suggests that the triplet spin densities on the C_{60} carbons in the crystal might well be half those on the C_{60} carbons in the solution. Consequently one is tempted to conclude that the triplet exciton concerns two buckyballs and we have calculated the ^{13}C ENDOR frequencies expected for a triplet excitation delocalized over two neighboring C_{60} molecules with a mutual orientation as for triplet γ and, as in the experiment, for a magnetic field parallel to the fine-structure x axis of this triplet. We attributed half of the spin densities given in Table 1 to the respective carbons of each C_{60} and calculated the ENDOR frequency of each ^{13}C from this ρ and the elements of A in Eq. [3] to which we added an isotropic hyperfine interaction a_{iso} which was treated as an adjustable parameter. The resulting ENDOR frequencies are represented as a stick spectrum in Fig. 6. With the magnetic field parallel to the x axis of triplet γ, the pair of C_{60} molecules contains 16 inequivalent atomic positions: 14 groups of 8 equivalent atoms and 2 groups of 4, hence 16 distinct ENDOR frequencies. The calculated ENDOR frequencies are spread over about 2.8 MHz, and this width depends only slightly on the value of a_{iso} (-30 MHz for the spectrum in Fig. 6). The calculated stick spectrum represents just a first step toward the simulation of the ENDOR spectrum. Nevertheless, the fact that the calculated spread of the

TABLE 1

Calculated Spin Densities on the Inequivalent Carbon Atoms of C_{60} in the Lowest Triplet State for a Distortion to D_{2h} Symmetry

	D_{2h}
Atom label	Spin density (%)
1	3.67
2	1.98
3	2.12
4	0.94
5	0.78
6	2.27
7	1.92
8	0.62
9	0.85

Note. The labels refer to the atom numbering in Fig. 5.

frequencies closely corresponds to that observed experimentally implies that the triplet excitation of the crystal is indeed delocalized over a pair of neighboring C_{60} molecules.

In summary, we have obtained 95-GHz pulsed ENDOR spectra of fully enriched $^{13}C_{60}$ in its triplet state at 1.2 K. The spectra for molecular $^{13}C_{60}$ in a decaline/cyclohexane glass show that the fine-structure parameter D is negative. The spectra for crystalline $^{13}C_{60}$ reveal that the triplet states of the crystal concern miniexcitons in which the excitation is delocalized over two neighboring C_{60} molecules. The ENDOR spectra represent fingerprints of the triplet-state wavefunction and the distortion of molecular and crystalline C_{60}. A full analysis requires the quantum-chemical study of the triplet spin-density distribution as a function of the molecular geometry and the calculation of the corresponding ENDOR frequencies. Preliminary results for a C_{60} molecule of D_{2h} symmetry, corresponding to the symmetry observed in the crystal, have been obtained and further work along these lines is in progress.

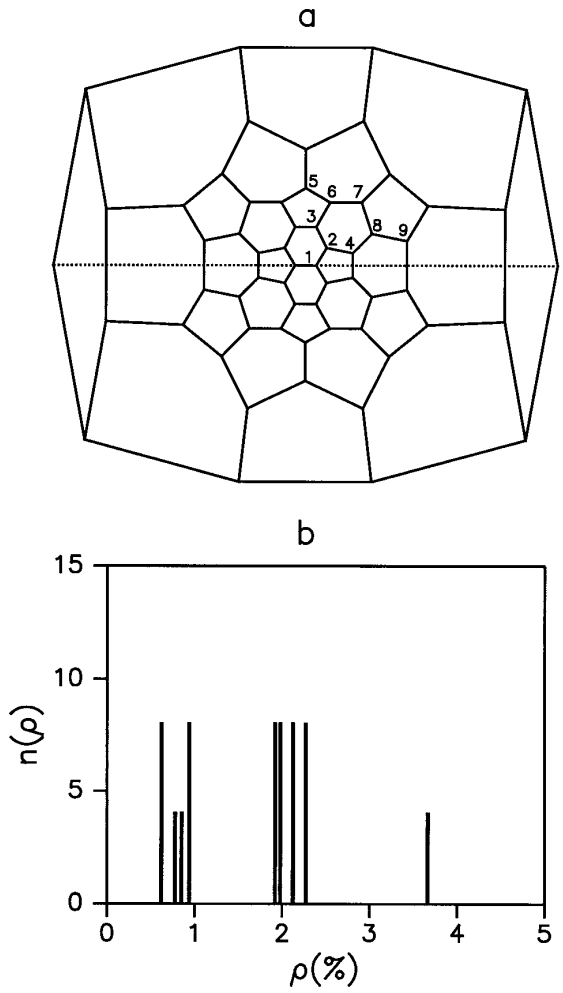

FIG. 5. (a) Schlegel representation of distorted C_{60} of D_{2h} symmetry. The numbers label the nine inequivalent carbon atoms. The central interpentagon bond corresponds to the bond labelled ''a'' in Ref. (5). (b) Stick diagram representing the number $n(\rho)$ of atoms with spin density ρ in the lowest triplet state of D_{2h}-distorted C_{60} according to MINDO calculations.

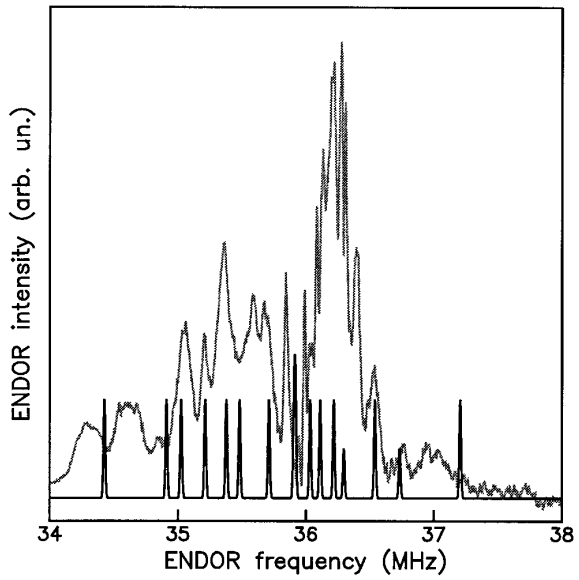

FIG. 6. Stick spectrum representing the $^{13}C_{60}$ ENDOR frequencies calculated for a triplet delocalized over a pair of $^{13}C_{60}$ molecules mutually oriented as in triplet γ at a field of 3.3776 T parallel to the fine-structure x axis. The isotropic hyperfine interaction parameter a_{iso} has been taken as -30 MHz (see text). For comparison the experimental ^{13}C-pulsed ENDOR spectrum of a single crystal at the same magnetic field strength and orientation (cf. Fig. 2) is reproduced in gray.

ACKNOWLEDGMENTS

We are indebted to Dr. M. C. van Hemert for his help with the quantum-chemical calculations. This work is supported by the Stichting voor Fundamental Onderzoek der Materie (FOM) with financial aid from the Nederlandse Organisatie voor Wetenschappelijk Onderzoek (NWO).

REFERENCES

1. R. D. Johnson, D. S. Bethune, and C. S. Yannoni, *Acc. Chem. Res.* **25,** 169 (1992).
2. R. Taylor, J. P. Hare, A. K. Abdul-Sada, and H. W. Kroto, *J. Chem. Soc., Chem. Commun.* **20,** 1423 (1990).
3. M. R. Wasielewski, M. P. O'Neill, K. R. Lykke, M. J. Pellin, and D. M. Gruen, *J. Am. Chem. Soc.* **113,** 2774 (1991).
4. I. László and L. Udvardi, *Chem. Phys. Lett.* **136,** 418 (1987); F. Negri, G. Orlandi, and F. Zerbetto, *Chem. Phys. Lett.* **144,** 31 (1988).
5. P. R. Surján, L. Udvardi, and K. Németh, *J. Mol. Struct. Theochem* **311,** 55 (1994).
6. A. Angerhofer, J. U. von Schütz, D. Widmann, W. H. Müller, H. U. ter Meer, and H. Sixl, *Chem. Phys. Lett.* **217,** 403 (1994).
7. A. Grupp, J. Pfeuffer, and M. Mehring, *in* ''Magnetic Resonance

and Related Phenomena'' (K. M. Salikhov, Ed.), Abstracts of the 27th Congress Ampere, Kazan, p. 967 (1994).

8. G. L. Closs, P. Gautam, D. Zhang, P. J. Krusic, S. A. Hill, and E. Wasserman, *J. Phys. Chem.* **96,** 5228 (1992).

9. X. L. R. Dauw, O. G. Poluektov, J. B. M. Warntjes, M. V. Bronsveld, and E. J. J. Groenen, *J. Phys. Chem.,* submitted.

10. A. Regev, D. Gamliel, V. Meiklyar, S. Michaeli, and H. Levanon, *J. Phys. Chem.* **97,** 3671 (1993).

11. P. R. Surján, K. Németh, M. Bennati, A. Grupp, and M. Mehring, *Chem. Phys. Lett.* **251,** 115 (1996).

12. M. Bennati, A. Grupp, and M. Mehring, *J. Chem. Phys.* **102,** 9457 (1995).

13. E. J. J. Groenen, O. G. Poluektov, M. Matsushita, J. Schmidt, J. H. van der Waals, and G. Meijer, *Chem. Phys. Lett.* **197,** 314 (1992).

14. M. Matsushita, A. M. Frens, E. J. J. Groenen, O. G. Poluektov, J. Schmidt, G. Meijer, and M. A. Verheijen, *Chem. Phys. Lett.* **214,** 349 (1993).

15. D. Zhang, J. R. Norris, P. J. Krusic, E. Wasserman, C.-C. Chen, and C. M. Lieber, *J. Phys. Chem.* **97,** 5886 (1993).

16. A. Grupp, J. Pfeuffer, and M. Mehring, *in* ''Electronic Properties of Novel Materials: Physics and Chemistry of Fullerenes and Derivates'' (H. Kuzmany, J. Fink, M. Mehring, and S. Roth, Eds.), p. 246, World Scientific, Singapore (1995).

17. I. Holleman, M. G. H. Boogaarts, P. J. M. van Bentum, and G. Meijer, *Chem. Phys. Lett.* **240,** 165 (1995).

18. J. A. J. M. Disselhorst, H. van der Meer, O. G. Poluektov, and J. Schmidt, *J. Magn. Reson. A* **115,** 183 (1995).

19. C. Gemperle, O. W. Sørensen, A. Schweiger, and R. R. Ernst, *J. Magn. Reson.* **87,** 502 (1990).

20. E. J. J. Groenen, W. J. Buma, and J. Schmidt, *Isr. J. Chem.* **29,** 99 (1989).

21. T. Cole and C. Heller, *J. Chem. Phys.* **34,** 1085 (1961).

22. A. Horsfield, J. R. Morton, J. R. Rowlands, and D. H. Whiffen, *Mol. Phys.* **5,** 241 (1962).

23. J. J. P. Stewart, MOPAC 93.00, Fujitsa Lim., Tokyo (1993).